Virus Research 269 (2019) 197640

Contents lists available at ScienceDirect

Virus Research

journal homepage: www.elsevier.com/locate/virusres

RNA silencing suppression mechanisms of *Triticum mosaic virus* P1: dsRNA binding property and mapping functional motifs

Adarsh K. Gupta[a,1], Satyanarayana Tatineni[b,*]

[a] Department of Plant Pathology, University of Nebraska-Lincoln, Lincoln, NE 68583, United States
[b] United States Department of Agriculture-Agricultural Research Service and Department of Plant Pathology, University of Nebraska-Lincoln, Lincoln, NE 68583, United States

ARTICLE INFO

Keywords:
Triticum mosaic virus
Poacevirus
P1
RNA silencing suppressor
dsRNA binding
GW-motif
Zinc-finger motif

ABSTRACT

Triticum mosaic virus (TriMV) is the exemplar strain of the type species of the genus *Poacevirus* in the family *Potyviridae* infecting wheat in the Great Plains region of the USA. Previously, we reported that the P1 protein of TriMV is a viral suppressor of RNA silencing. Mutational analyses of P1 showed that deletion of 55 N-terminal amino acids, and a single amino acid at the C-terminus retained its ability to suppress ssGFP-induced RNA silencing. These data suggest that the N-terminal region but not the C-terminal region of P1 is flexible for suppression of RNA silencing activity. Computational analyses revealed that TriMV P1 contains LXK/RA and zinc finger motifs at the N-terminal region and a domain containing the GW motif at the C-terminal region. Mutational analysis of TriMV P1 suggested functional roles for these motifs in suppression of RNA silencing. Electrophoretic mobility shift assays with bacterially expressed P1 protein revealed that P1 binds to 180-nt and 21- and 24-nt ds-siRNAs derived from green fluorescent protein sequence. Additionally, TriMV P1 protected the 655-nt long dsRNA derived from TriMV coat protein from dicing by the human Dicer enzyme into siRNAs. Disruption of the GW motif in TriMV P1 with a W332A mutation abolished silencing suppression, pathogenicity enhancement and viability of TriMV, suggesting a functional role for the GW motif in suppression of RNA silencing.

1. Introduction

RNA silencing is sequence-specific degradation of target RNAs by a protein called Argonaute (AGO), guided by complementary short-interfering RNAs (siRNAs) that are produced by the dsRNA-specific endoribonuclease activity of dicer-like enzymes, DCL (Baulcombe, 2004; Ding and Voinnet, 2007; Hamilton and Baulcombe, 1999; Meister and Tuschl, 2004). RNA genomes of viruses and their replicative double-stranded RNAs (dsRNAs) (Meister and Tuschl, 2004; Xie et al., 2001) are trigger and substrate of RNA silencing, attributing an antiviral defensive nature to post-transcriptional gene silencing in plants and a few groups of animals and fungi (Covey et al., 1997; Csorba et al., 2015; Fire et al., 1998; Ratcliff et al., 1997; Romano and Macino, 1992; Ullu et al., 2004). Besides dsRNA molecules, RNA silencing can also be triggered by overexpressed transgenes (Béclin et al., 2002), class-I transposons (Buchon and Vaury, 2006), repetitive elements (Siomi et al., 2011), imperfect stem-loops (Bartel, 2004), or self-complementary fold-backs (Chuang and Meyerowitz, 2000). To circumvent or counteract the effects of host-defensive RNA silencing, viruses encode suppressors of RNA silencing (Csorba et al., 2015; Li and Ding, 2006; Roth et al., 2004).

Viral suppressors of RNA silencing (VSRs) mount counterdefensive responses by targeting specific players or events of RNA silencing. Pothos latent virus-encoded P14 protein (Mérai et al., 2005), P38 capsid protein of turnip crinkle virus (TCV; Mérai et al., 2006), or tomato spotted wilt virus NSs protein (Schnettler et al., 2010) were shown to bind to dsRNA. TCV P38 or rice yellow mottle virus P1 protein (Lacombe et al., 2010) was shown to directly inhibit the activity of DCL4 (Deleris et al., 2006). Tombusviral P19 protein (Silhavy et al., 2002) or cucumber mosaic virus 2b protein (Diaz-Pendon et al., 2007) sequesters siRNA to interfere in the process of siRNA loading in RISC formation as well as in intercellular systemic mobility of silencing signals. Sweet potato mild mottle virus (SPMMV) P1 protein blocks AGO protein to halt downstream functions of RISC (Giner et al., 2010). Conversely, P25 protein of potato virus X (PVX) tags AGO for ubiquitin/26S proteasome system-mediated degradation (Chiu et al., 2010). The

* Corresponding author.
E-mail address: satyanarayana.tatineni@ars.usda.gov (S. Tatineni).
[1] Present address: Department of Entomology, Texas A&M University, College Station, TX 77843, United States.

https://doi.org/10.1016/j.virusres.2019.197640
Received 1 May 2019; Received in revised form 8 June 2019; Accepted 14 June 2019
Available online 17 June 2019
0168-1702/ Published by Elsevier B.V.

P6 protein of rice yellow stunt virus interacts with RDR6 to suppress the transient pathway of RNA silencing (Guo et al., 2013). HC-Pro is one of the first characterized VSRs of potyviruses, which suppress RNA silencing through a variety of methods such as sequestration of siRNAs, binding and inactivation of HEN1, and down regulation of RDR6 (Anandalakshmi et al., 1998; Kasschau and Carrington, 1998; Valli et al., 2018). Additionally, species like cucurbit vein yellowing virus (CVYV) which lacks HC-Pro employ its P1b protein as its silencing suppressor (Valli et al., 2006). However, SPMMV and wheat streak mosaic virus (WSMV) employ P1 as their VSRs despite having a functional HC-Pro (Giner et al., 2010; Young et al., 2012). Recently, the trans-frame gene P1N-PISPO of sweet potato feathery mottle virus, a potyvirus, has been reported as a suppressor of RNA silencing (Mingot et al., 2016; Untiveros et al., 2016).

Triticum mosaic virus (TriMV), the exemplar strain of the type species of the genus *Poacevirus* in the family *Potyviridae* (Fellers et al., 2009; Tatineni et al., 2009), is an economically important virus of wheat in the Great Plains region of the United States (Burrows et al., 2009). In synergistic interactions with other eriophyid-mite transmitted viruses such as WSMV and High Plains wheat mosaic virus, TriMV can cause enhanced disease with severe yield loss in winter wheat (Byamukama et al., 2012, 2013). VSRs play a pivotal role in virus-host interactions given the fact that they directly determine the fate of a virus starting from the site of invasion to the establishment of stable systemic infection. Studying silencing suppressors of economically important viruses bolsters our understanding of virus-host interactions for the development of new disease management strategies. Previously, we showed that TriMV-encoded P1, a type B P1 protein (Rodamilans et al., 2013), efficiently suppressed local and systemic RNA silencing induced by ssRNA or dsRNA *in planta* and enhanced pathogenicity of a heterologous virus (Tatineni et al., 2012). However, there is no information on the mechanisms of P1 RNA silencing suppression and the minimal region and domains or motifs in TriMV P1 that are required.

In this report, we show that 55 amino acids (aa) at the N-terminus and a single aa at the C-terminus of TriMV P1 are expendable for VSR function. P1 harbors conserved LXK/RA and zinc finger motifs toward the N-terminal region that are required for suppression of RNA silencing function. Electrophoretic mobility shift assays revealed that P1 binds to dsRNAs in a sequence independent manner and sequesters ds-siRNAs. Additionally, we found that TriMV P1 interferes with the process of dsRNA dicing into siRNAs *in vitro*. A single GW dipeptide motif is present toward the C-terminal region of P1 and mutagenesis of this motif resulted in the loss of silencing suppression activity and pathogenicity enhancement.

2. Materials and methods

2.1. Generation of constructs

The N- and C-terminal deletion and point mutants of TriMV P1 were created using pTriMV-R (Tatineni et al., 2015) as a template for overlap extension PCR. Deletion and point mutants were named based on the direction or location of mutagenesis. For example, ΔN40 represents P1 lacking N-terminal 40 amino acids. For agroinfiltration-based transient expression, P1 or its mutants were cloned under a double CaMV 35S promoter in pCASS4 plasmid (a variant of pCASS2; Shi et al., 1997) along with the 5'-NTR of tobacco etch virus (TEV) as translation enhancer sequence (Carrington and Freed, 1990). pCASS4-TriMV P1 constructs were chemically transformed into *Agrobacterium tumefaciens* strain EHA105. For bacterial overexpression, P1 or P1-W332A cistron was ligated into pMAL-c5X between *Not*I and *Bam*HI restriction sites and chemically transformed into *Escherichia coli* strain NEB Express (New England Biolabs Inc., Ipswich, MA). For chimeric expression of P1 or P1-W332A in PVX, PCR-amplified sequences were inserted into PVX infectious clone (Chapman et al., 1992) between *Asc*I and *Cla*I restriction enzyme sites. A single point mutation of W332A was introduced in GFP-tagged TriMV infectious clone (TriMV-GFP; Tatineni et al., 2015) to generate TriMV-GFP-P1-W332A. Sequences of all constructs were verified by sequencing on 3730xl DNA Analyzer (Applied Biosystems, Foster City, CA) at the University of Florida ICBR Core DNA sequencing facility.

2.2. Agroinfiltration assay

A. tumefaciens harboring pCASS4 constructs of P1 mutants were suspended in infiltration buffer containing 10 mM $MgCl_2$, 10 mM MES, pH 5.5, 100 μM Acetosyringone to an optical density of 1.0 at 600 nm. Following 3 h incubation at room temperature, the agrosuspension was mixed with an equal volume of agrobacterial cells containing 35S:ssGFP (Qu et al., 2003) as a reporter and infiltrated into fully expanded leaves of GFP transgenic *N. benthamiana* line 16c leaves at the 6–8 leaf stage (Voinnet and Baulcombe, 1997). Infiltrated plants were maintained in a growth chamber at 24–26 °C with a photoperiod of 14 h. Infiltrated leaves were observed for green fluorescence under long range UV light at 5 or 7 days postagroinfiltration (dpa) and photographed using Nikon D70 DSLR camera (Nikon, Melville, NY). Two independent clones per mutant were analyzed for suppression of RNA silencing assay in 2–3 independent experiments, and representative results from one experiment were presented.

2.3. RNA extraction and blotting

Following observations under UV light, infiltrated regions of *N. benthamiana* leaves were excised for total RNA extraction by TriPure isolation method (Roche, Indianapolis, IN). Total RNA (2 μg) was subjected to electrophoresis through 1% agarose-formaldehyde gel or 15% urea-polyacrylamide gel and transferred onto a positively charged nylon membrane and probed for GFP specific mRNA or siRNA using digoxigenin (DIG)-labelled riboprobes as described in Tatineni et al. (2012).

2.4. Electrophoretic mobility shift assay

Double-stranded RNA was prepared by annealing *in vitro* transcripts of GFP (180-nt corresponding to the 5' end of GFP) or TriMV CP (655-nt corresponding to nts 9326-9980 of TriMV genome) in 20 mM Tris-HCl (pH 8.0), 1 mM EDTA, 50 mM NaCl and 0.02% Tween 20 (TEN-T buffer). Chemically synthesized 21- or 24-nt 5'P-oligoribonucleotides were annealed in 20 mM Tris-HCl (pH 8.0), 1 mM EDTA and 50 mM NaCl (TEN buffer) to generate ds-siRNA with 2-nt 3' overhangs. Recombinant maltose binding protein (MBP)-tagged TriMV P1 or TriMV P1-W332A was expressed in *E. coli* transformed with pMAL-c5X constructs and affinity purified using amylose resin (New England Biolabs, Ipswich, MA). Affinity purified MBP::P1 or MBP::P1-W332A proteins were quantified by Bradford method. Five μg of purified recombinant P1 or P1-W332A was incubated with 180-nt dsRNA (100 ng) or 21- and 24-nt ds-siRNAs (50 ng each) in a 30-μl reaction at room temperature for 30 min. The reaction mix was resolved through a non-denaturing PAGE at 4 °C, followed by SYBR Green staining (Thermo Scientific, Waltham, MA) as described in Samuel et al. (2016).

2.5. In vitro dicing assay

Five hundred ng of 655-nt long dsRNA was incubated with 0.5 U of recombinant human Dicer enzyme (Turbo Dicer siRNA generation kit, Genlantis, San Diego CA) along with 0.3 nmol of bacterial expressed MBP::P1 or MBP at 37 °C in a 30 μL reaction. Following incubation as per manufacturer's guidelines, the reaction was stopped with 10 mM EDTA and subjected to non-denaturing PAGE analysis at 4 °C, followed by SYBR Green staining. MBP supplemented reaction was used as a non-VSR protein control as well as a negative control for MBP affinity tags.

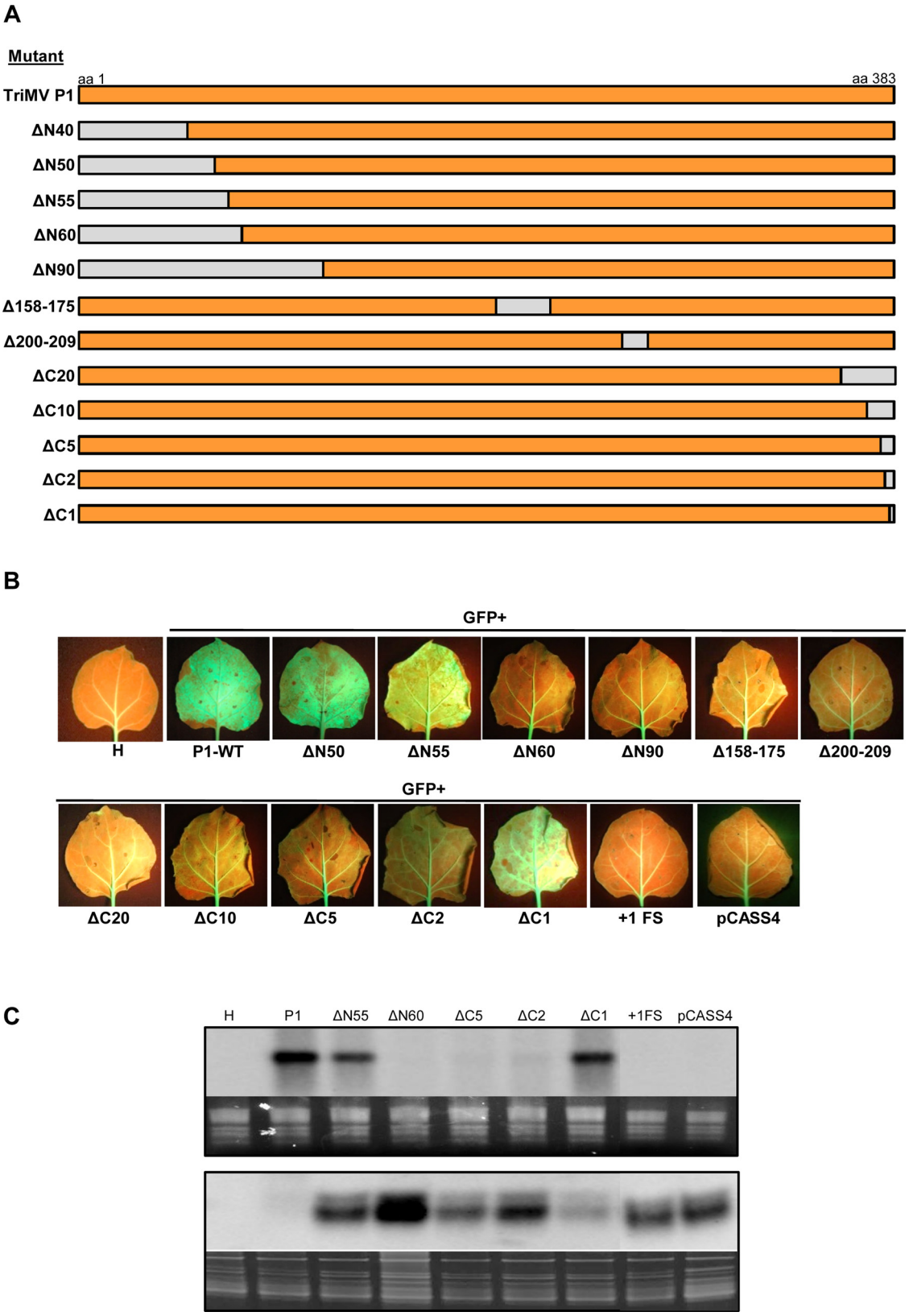

Fig. 1. Mapping the minimal region of Triticum mosaic virus (TriMV) P1 required for suppression of ssGFP-induced local RNA silencing. (A) Schematic representation of deletion mutants of TriMV P1. Deleted regions are indicated with gray. TriMV P1 sequences with deletions were cloned into pCASS4 under a double 35S promoter. (B) Green fluorescence images of *N. benthamiana* 16c leaves agroinfiltrated with TriMV P1 deletion mutants plus 35S:ssGFP at 5 days post-agroinfiltration (dpa). Image H indicates uninfiltrated healthy leaf; Image pCASS4 indicates co-infiltration of pCASS4 and 35S:ssGFP as a negative control. Green fluorescence indicates successful expression of GFP reporter upon suppression of RNA silencing, while red auto-fluorescence indicates silencing of GFP reporter. (C) Northern blot hybridization of total RNA extracted from agroinfiltrated regions of select constructs showing accumulation of GFP specific mRNA (upper panel) and siRNAs (lower panel) at 5 dpa. Ethidium bromide stained gels showing the amount of RNA loaded.

2.6. Mutant or chimeric viral infections

The P1 cistron with W332A mutation was introduced into pTriMV-GFP through overlap PCR to obtain pTriMV-GFP-P1-W332A. *In vitro* transcripts of TriMV-GFP or TriMV-GFP-P1-W332A were inoculated onto wheat cv. Tomahawk seedlings at the single leaf stage as described in Tatineni et al. (2011). Inoculated leaves at 10 and 21 dpi and upper noninoculated leaves at 21 dpi were observed under Zeiss Stereo Discovery V12 Fluorescence Microscope with a narrow-band GFP filter. *In vitro* transcripts of PVX, PVX-TriMV-P1, or PVX-TriMV-P1-W332A were inoculated onto fully expanded leaves of *N. benthamiana* at the 6-leaf stage. Inoculated plants were maintained at 25 °C in a growth chamber with a 16 h photoperiod, and plants were observed for PVX pathogenicity. Total RNA was extracted from upper noninoculated leaves at 10 and 15 dpi for RT-PCR and RT-qPCR analyses.

2.7. RT-PCR and RT-qPCR

TriMV-GFP, TriMV-GFP-P1-W332A, or buffer inoculated wheat plants were subjected to total RNA isolation from inoculated (10 and 21 dpi) or upper noninoculated (21 dpi) leaves by glycine-phenol method (McNeil et al., 1996). Total RNA was reverse transcribed with random primers using SuperScript III First-Strand Synthesis System (Invitrogen, Carlsbad, CA), followed by PCR for TriMV P1 amplification. Total RNA was extracted from PVX symptomatic *N. benthamiana* leaves inoculated with PVX-TriMV-P1 or PVX-TriMV-P1-W332A at 10 and 15 dpi using Tripure isolation reagent, followed by RT-PCR with primers Tr-206 and Tr-207 (Gupta et al., 2018). Real-time RT-PCR (RT-qPCR) was performed on total RNA extracted from two biological replicates of PVX-infected symptomatic top leaves at 10 and 15 dpi with primers G-35 and G-36 as described in Gupta et al. (2018) using SsoAdvanced SYBR Green Supermix (Bio-Rad) on Bio-Rad CFX Connect Real-Time PCR System. Relative expression of PVX transcripts was determined by ΔΔCt method against an internal reference of *N. benthamiana* actin, and fold change was calculated based on relative expression of PVX-WT.

2.8. Western blotting

Total proteins were extracted from TriMV-GFP-, TriMV-GFP-P1-W332A-, or buffer-inoculated wheat leaves as described in Tatineni et al. (2011). Total proteins were boiled in 1X Laemmli buffer and size separated on 15% SDS-PAGE and transferred onto PVDF membrane for immunoblotting with anti-GFP monoclonal antibody (Clontech, Mountain View, CA) or anti-TriMV CP polyclonal antiserum (Tatineni et al., 2013).

2.9. In silico analyses

GenBank sequences of type B P1 sequences of potyvirid species (Rodamilans et al., 2013) were manually trimmed and analyzed for homology of regions of interest by multiple sequence alignment with deep substitution scoring matrix, BLOSUM62 (Henikoff, 1992). ExPASy ProtScale program was used to generate a Kyte-Doolittle hydropathy plot for a conserved domain containing GW dipeptide (Kyte and Doolittle, 1982). Prediction of secondary structure was performed by Chou-Fasman method (Chou and Fasman, 1974).

3. Results

3.1. Mapping the minimal region required for RNA silencing suppression activity of TriMV P1

We previously reported that the P1 protein, which constitutes 383 out of 3112 N-terminal amino acids of polyprotein encoded by the TriMV genome is a suppressor of RNA silencing (Tatineni et al., 2012). In this study, deletion mutation analysis of P1 was performed to determine the minimal region required for VSR activity. A total of ten terminal deletion mutants, five deletions each from the N- and C-terminal regions, and two internal deletion mutants were engineered in the P1 cistron (Fig. 1A), followed by ligation into pCASS4 between the double 35S promoter and a terminator.

N. benthamiana line 16c leaves infiltrated with P1 harboring deletions of up to 50 N-terminal amino acids showed efficient VSR with prolonged green fluorescence at 5 dpa similar to wild-type P1. However, when deletions extended to 55 N-terminal amino acids, the VSR function of P1 was substantially reduced compared with wild-type P1 (Fig. 1B). In contrast, only a single aa at the C-terminus was dispensable for efficient suppression of RNA silencing. Deletions beyond 55 amino acids from the N-terminus and two internal deletions (Δ158-175 and Δ200-209) completely abolished the suppression of RNA silencing function, similar to that of empty pCASS4 and TriMV P1 with a +1 frameshift mutation (Fig. 1B). Northern blot hybridizations were performed on total RNA isolated from infiltrated regions to detect GFP specific mRNA and siRNAs at 5 dpa. N-terminal deletion of 55 amino acids showed reduced levels of GFP specific mRNA with increased accumulation of siRNAs compared to wild-type P1 (Fig. 1C, compare lane N55 with lane P1). Accumulation of GFP-specific siRNAs was higher in P1 with deletions comprising 55 or more amino acids from the N-terminal region and deletions of more than 2 amino acids from the C-terminal region, similar to that of TriMV P1 with a +1 frameshift and pCASS4 controls (Fig. 1C; data not shown). These data revealed that 55 amino acids from the N-terminal region and a single amino acid from the C-terminal region are dispensable for VSR activity of TriMV P1.

3.2. The LXK/RA motif and a putative zinc-finger domain are required for VSR function of TriMV P1

Sequence comparison of TriMV P1 with other type B P1 sequences of potyvirid species revealed the presence of an LXK/RA motif (aa 91-94) and a putative zinc-finger domain (aa 110-130) with remarkable sequence conservation (Fig. 2A). The requirement of these domains in suppression of RNA silencing was examined by alanine scanning of select amino acids of TriMV P1 (Fig. 2B). The functional significance of LXK/RA motif (aa 91-94) in TriMV P1 was examined by mutating L91A and LR92/93AA, followed by suppression of RNA silencing assay by co-agroinfiltration with 35S:ssGFP. Mutation of L91A maintained VSR function, while LR92/93AA completely lost the ability to suppress RNA silencing in terms of expression of GFP reporter at 7 dpa (Fig. 2C). These data suggest that LXK/RA motif is critical for VSR function.

We next examined the significance of the putative zinc-finger domain of TriMV P1 by mutating C110, C113, C116, H127, and C130 residues to alanine, followed by ligation into pCASS4. RNA silencing suppression ability of these mutants was examined by co-agroinfiltration with 35S:ssGFP into *N. benthamiana* 16c leaves. Expression of GFP reporter in agroinfiltrated leaf patches with mutants C110A, C113A, H127A, or C130A was drastically reduced at 7 dpa, suggesting that these amino acids are required for suppression of RNA silencing activity (Fig. 2C). In contrast, mutation of non-conserved C116 in TriMV P1 did not affect suppression of local RNA silencing (Fig. 2C). Previous studies on CVYV P1b showed that mutation of amino acids in conserved LXKA and putative zinc-finger domains abolished the suppression of RNA silencing (Valli et al., 2008).

We next examined the requirement of predicted serine protease domain (aa 286-383) of P1 for suppression of RNA silencing activity by individually mutating three of the predicted catalytic triad residues, H286, D301, and S333 (Ryan and Flint, 1997). These catalytic triad residues of P1 cistrons of potyvirid species are required for proteinase activity (Valli et al., 2008; Verchot et al., 1991, 1992). TriMV P1 mutants H286A, D301A, or S333A were co-agroinfiltrated with 35S:ssGFP, and it was found that mutant H286A failed to suppress RNA silencing, while mutants D301A and S333A efficiently suppressed RNA silencing. These results suggest that serine proteinase activity of P1 is not required

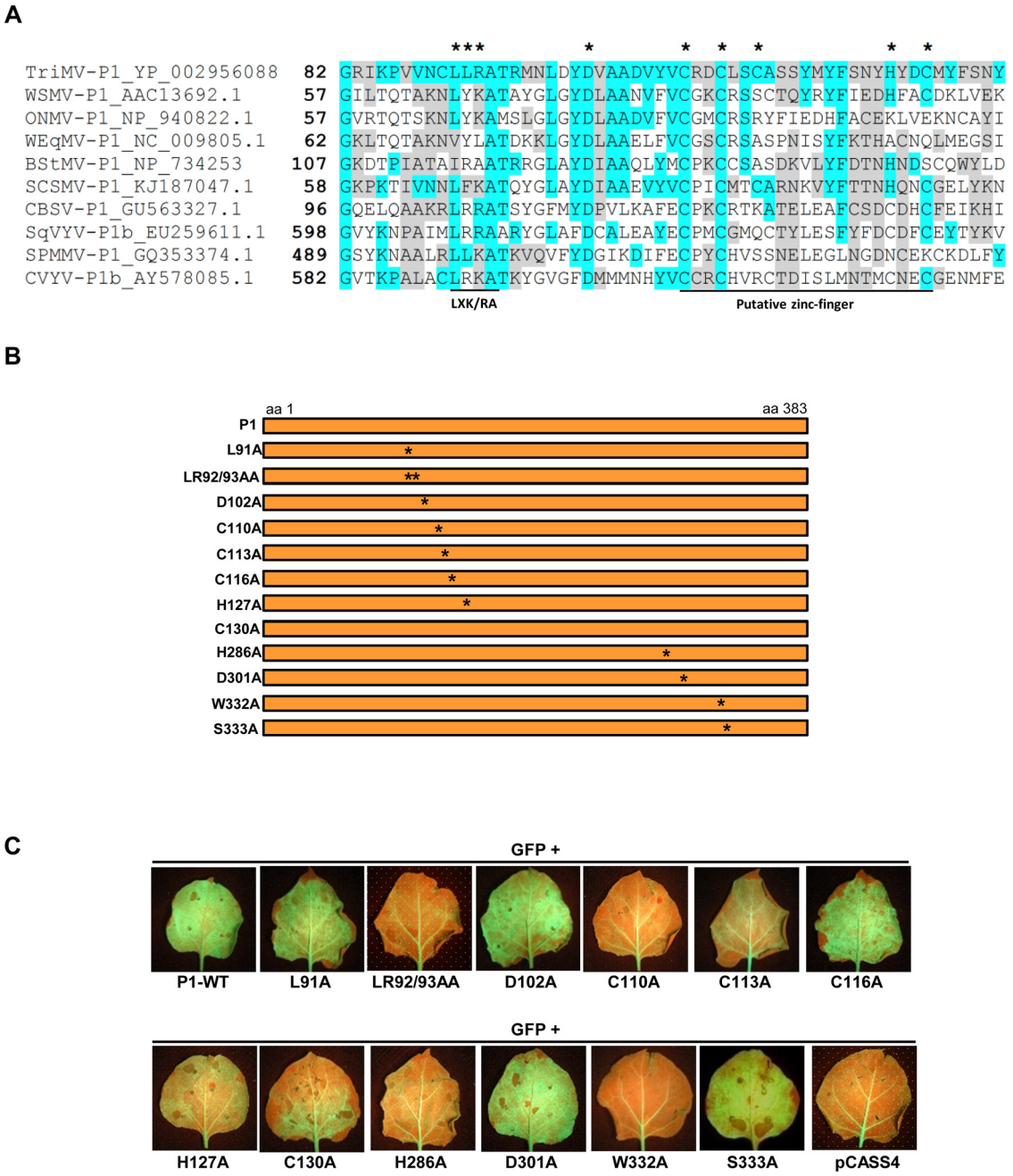

Fig. 2. Conserved domains in Triticum mosaic virus (TriMV) P1 are required for suppression of RNA silencing. (A) Multiple sequence alignment of type B P1 partial sequences of TriMV, wheat streak mosaic tritimovirus (WSMV), oat necrotic mottle tritimovirus (ONMV), wheat eqlid mosaic tritimovirus (WEqMV), brome streak mosaic tritimovirus (BStMV), sugarcane streak mosaic poacevirus (SCSMV), cassava brown streak ipomovirus (CBSV), squash vein yellowing ipomovirus (SqVYV), sweet potato mild mottle ipomovirus (SPMMV), and cucumber vein yellowing ipomovirus (CVYV). GenBank accession numbers of each viral protein was indicated in the sequence identifier along with the position of the first residue of each sequence in boldface. Identical amino acids were highlighted in turquoise indicating high conservation, and amino acids with similar biochemical properties were highlighted in gray. Location of LXK/RA and putative zinc-finger domain is indicated. (B) Schematic diagrams of TriMV P1 cistron with the location of point mutations (in asterisks). TriMV P1 sequences with point mutations were cloned in pCASS4 and were co-agroinfiltrated with 35S:ssGFP. (C) Green fluorescence images of *N. benthamiana* 16c leaves agroinfiltrated with TriMV P1 point mutants plus 35S:ssGFP at 7 days postagroinfiltration. Image pCASS4 indicates co-infiltration of pCASS4 and 35S:ssGFP as a negative control.

for VSR function.

3.3. TriMV P1 binds to dsRNA but not to ssRNA

We next examined whether TriMV P1 possesses dsRNA binding property as reported for other VSRs (Lakatos et al., 2006; Mérai et al., 2006). The P1 cistron of TriMV was engineered into pMAL-c5X, and expressed *in vitro* in *E. coli* as MBP-tagged P1 (Fig. 3A, lane 2). The dsRNA binding property of TriMV P1 was examined by incubating MBP::P1 with GFP-specific *in vitro* synthesized 180-nt long dsRNA or chemically synthesized 21- and 24-nt ds-siRNAs. Analysis of protein-RNA interaction reactions through native PAGE, followed by SYBR Green staining (Samuel et al., 2016) revealed that dsRNA or ds-siRNAs formed complexes with MBP::P1 but not with MBP when compared to dsRNA-only control (Fig. 3B, C; compare lanes 1 with lanes 3 and 4). Complexes formed between dsRNA and protein resulted in an electrophoretic mobility shift with MBP::P1 but no such shifts were observed with MBP (Fig. 3B, C, compare lane 1 with lane 3). These results

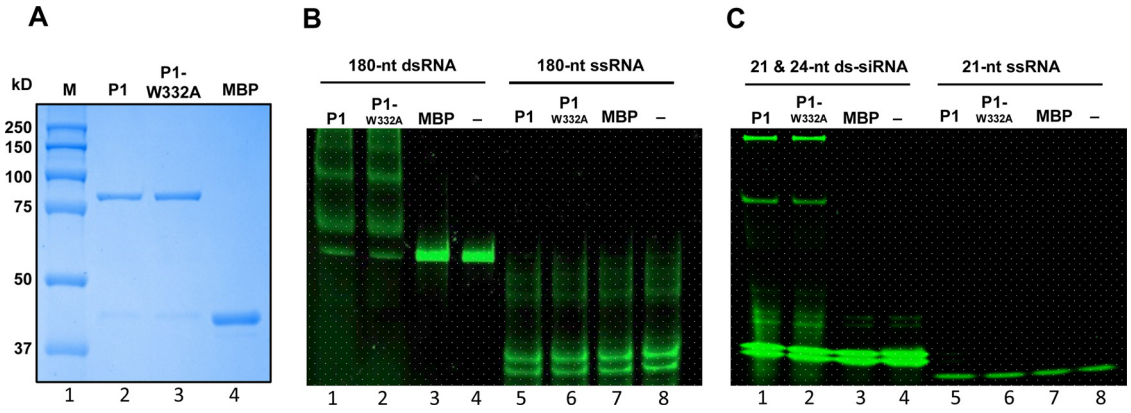

Fig. 3. Triticum mosaic virus (TriMV) P1 binds to double-stranded (ds) RNAs in electrophoretic mobility shift assay. (A) Coomassie Brilliant Blue R-250-stained SDS-PAGE of bacterially expressed and affinity-purified MBP::P1 (lane 2), MBP::P1-W332A (lane 3) and MBP (lane 4). Lane 1 (M) shows protein standard. (B & C) Electrophoretic mobility shift assay of TriMV P1 (lanes 1 and 5) or P1-W332A (lanes 2 and 6) incubated with GFP-derived 180-nt (B, lanes 1–4), 21- and 24-nt ds-siRNAs (C, lanes 1–4), 180-nt ssRNA (B, lanes 5–8), or 21-nt ssRNA (C, lanes 5–8). Note the retarded electrophoretic mobility of dsRNAs but not ssRNAs incubated with P1 or P1-W332A compared with MBP. MBP was used as a non-viral suppressor of RNA silencing protein control and the affinity tag of test proteins.

indicate that TriMV P1 binds to dsRNA in a size-independent manner.

The binding ability of TriMV P1 to ssRNA was examined by incubating MBP::P1 with *in vitro* synthesized GFP-specific 180-nt or 21-nt ssRNA followed by native PAGE. TriMV P1 did not form complexes with ssRNAs of 180-nt or 21-nt as ssRNAs incubated with MBP::P1 resolved in PAGE similar to those of MBP or ssRNA-only control samples (Fig. 3B, C, compare lanes 5 with lanes 7 and 8). These data revealed that TriMV P1 does not bind to ssRNAs of 180-nt or 21-nt at detectable levels.

3.4. TriMV P1 protects dsRNA from dicing

The above RNA-protein interaction studies revealed that TriMV P1 possesses dsRNA binding property, which has been shown to have functional significance in protecting dsRNAs from dicing (Mérai et al., 2006). *In vitro* siRNA generation experiment was performed by using recombinant human Dicer on a 655-nt long dsRNA derived from TriMV CP in the presence of MBP::P1 or MBP. As presented in Fig. 4, dicing of 655-nt long dsRNA into siRNAs by human Dicer was inhibited in the presence of MBP::P1. Additionally, dsRNA in a dicing reaction supplemented with MBP::P1 showed retarded electrophoretic mobility with substantially reduced accumulation of diced siRNAs compared with MBP or buffer supplemented dicing reactions (Fig. 4, compare lane 1 with lanes 2 and 3). These results indicate that the dsRNA binding property of P1 aids suppression of RNA silencing through protection of dsRNAs and inhibition of RISC formation through siRNA sequestration.

3.5. The GW motif of TriMV P1 is required for suppression of ssRNA-induced local silencing

Analysis of TriMV P1 amino acid sequence revealed the presence of a conserved glycine-tryptophan (GW) dipeptide motif at the C-terminal region (Fig. 5A). The domain harboring this GW dipeptide motif showed exceptional conservation with other type B P1 proteins of potyvirid species (Fig. 5A). Further analyses of the GW-motif harboring domain showed a hydropathy score of 0.6 through Kyte-Doolittle method, and secondary structure prediction of the GW domain suggested that the GW peptide is oriented toward the edge of its β-sheet (Fig. 5B).

Previous studies identified the significance of WG/GW dipeptide motifs in AGO interactions for suppression of RNA silencing (Bies-Etheve et al., 2009; Giner et al., 2010; Szabó et al., 2012). We introduced W332A mutation to examine the significance of the GW motif in suppression of RNA silencing (Fig. 2B). Agroinfiltration of 35S:P1-W332A along with 35S:ssGFP into the leaves of *N. benthamiana* 16c at

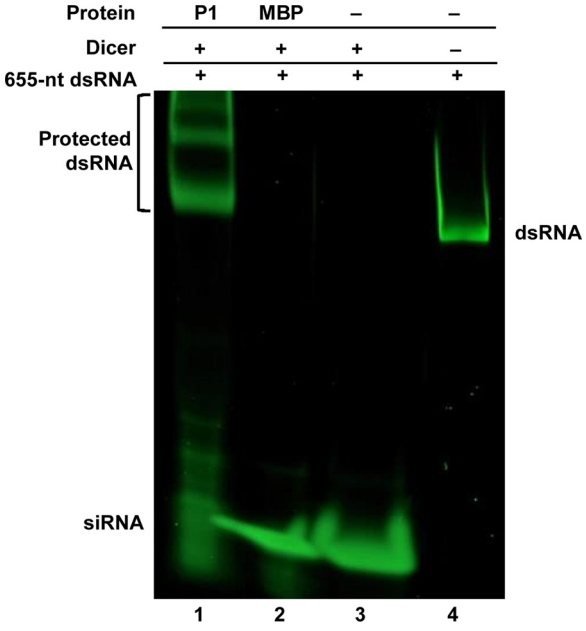

Fig. 4. Triticum mosaic virus (TriMV) P1 interferes with dicer activity on dsRNA. Dicing reaction on *in vitro* synthesized 655-nt long dsRNA was performed with recombinant human Dicer supplemented with MBP::P1 (lane 1) or MBP (lane 2) or buffer (lane 3) resolved on non-denaturing PAGE. Note dsRNA protection visualized as electrophoretic mobility shift against dicer activity and reduced accumulation of siRNA in MBP::P1 supplemented reaction, but not with MBP or buffer (no protein). MBP was included as a non-viral suppressor of RNA silencing protein control as well as a negative control for MBP affinity tag of MBP::P1. Lane 4 visualizes 100 ng of 655-nt dsRNA loaded as size marker and no-dicer dsRNA-only control.

the 6–8 leaf stage resulted in no green fluorescence at 5 dpa (data not shown) or 7 dpa (Fig. 2C). These data suggest that the GW motif of TriMV P1 plays a major role in suppression of ssRNA-induced local RNA silencing.

To test whether disruption of the GW motif affects dsRNA binding property of P1, 180-nt dsRNA or 21- and 24-nt ds-siRNAs were incubated with bacterially expressed MBP::P1-W332A protein (Fig. 3A, lane 3). The binding reactions of MBP::P1-W332A with dsRNAs was analyzed on a native PAGE, and it was found that P1-W332A formed complexes with GFP-specific 180-nt dsRNA or 21- and 24-nt ds-siRNAs, similar to that of wild-type P1 (Fig. 3B,C, compare lanes 2 with lanes 1). Similar to MBP::P1, MBP::P1-W332A did not form complexes with GFP-

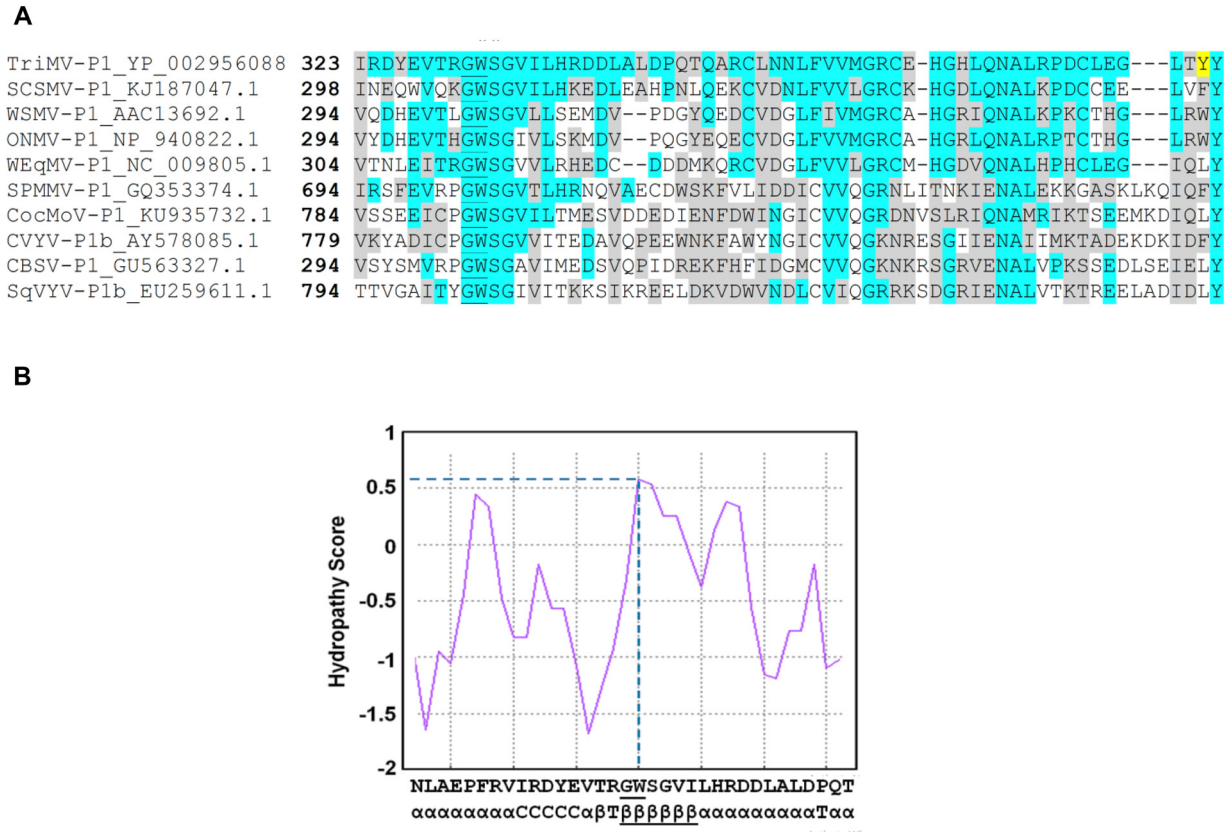

Fig. 5. Triticum mosaic virus (TriMV) P1 harbors a GW-containing domain. (A) Multiple sequence alignment of C-terminal regions of type B P1 sequences of TriMV, SCSMV, WSMV, ONMV, WEqMV, SPMMV, CocMoV, CVYV, CBSV, and SqVYV. The location of the GW dipeptide motif is underlined. Blocks of similar amino acids and amino acids with similar biochemical properties were highlighted in turquoise and gray, respectively. (B) Hydrophilicity plot and conceptual secondary structure of the GW motif-containing region of TriMV P1. Note solubility of GW and formation of a unique β-sheet is required for intermolecular interactions.

specific 180-nt or 21-nt ssRNA molecules at detectable levels (Fig. 3B,C, compare lanes 6 with lanes 5). Collectively, these data suggest that the GW motif of TriMV P1 is not required for dsRNA binding property for VSR function.

3.6. Disruption of the GW motif in TriMV P1 fails to enhance pathogenicity of a heterologous virus

We have previously demonstrated the pathogenicity enhancement property of TriMV P1 through chimeric expression in PVX on *N. benthamiana* (Tatineni et al., 2012). To determine the significance of the GW motif in pathogenicity enhancement of P1, P1-W332A sequence was engineered in pT7-P2C2S-PVX (Chapman et al., 1992). *N. benthamiana* plants inoculated with *in vitro* transcripts of PVX-WT, PVX-TriMV-P1, or PVX-TriMV-P1-W332A elicited mosaic symptoms with leaf curling at 8 days postinoculation (dpi). However, at 15 dpi, plants inoculated with PVX-TriMV-P1 exhibited severe apical necrosis resulting in stunted growth. Plants inoculated with PVX-TriMV-P1-W332A or PVX-WT showed remarkable symptom recovery with mild mosaic symptoms (Fig. 6A). RT-PCR analysis from total RNA extracted from symptomatic leaves at 15 dpi with primers flanking the location of chimeric insertion in the PVX genome showed stable inserts with expected size (Fig. 6B). Relative expression of PVX transcripts was assayed by RT-qPCR in total RNA extracted from symptomatic leaves at 10 and 15 dpi. Relative expression of PVX-TriMV-P1-W332A upon normalization with Nb-Actin reference gene revealed a 21- and 39-fold decrease in comparison with PVX-TriMV-P1 at 10 and 15 dpi, respectively. Moreover, relative expression of PVX-TriMV-P1-W332A in *N. benthamiana* was similar to that of PVX-WT at 10 and 15 dpi (Fig. 6C), suggesting that the GW motif is required for pathogenicity enhancement.

3.7. Disruption of the GW motif in P1 cistron is lethal to TriMV

We next examined the requirement of the GW motif in P1 cistron for the viability of TriMV by mutating W332A in a GFP-tagged TriMV cDNA clone (pTriMV-GFP) to generate pTriMV-GFP-P1-W332A (Fig. 7A). *In vitro* transcripts of TriMV-GFP-P1-W332A or TriMV-GFP were inoculated onto wheat seedlings at the single leaf stage. At 10 and 21 dpi, fluorescence microscopic analysis of inoculated leaves revealed the formation of foci only on TriMV-GFP-inoculated wheat leaves (Fig. 7B). At 21 dpi, upper noninoculated leaves showed systemic infection in wheat inoculated with TriMV-GFP but not with TriMV-GFP-P1-W332A (Fig. 7B). RT-PCR analysis on total RNA revealed that expected PCR product was obtained only from TriMV-GFP inoculated (10 and 21 dpi) and upper noninoculated (21 dpi) leaves but not in TriMV-GFP-P1-W332A- or buffer-inoculated wheat samples (Fig. 7C). Western blot analysis on total proteins extracted from inoculated leaves at 10 and 21 dpi and upper noninoculated leaves at 21 dpi revealed the presence of CP and GFP proteins only in TriMV-GFP-inoculated plants (Fig. 7D). These data suggest that the GW motif in P1 is crucial for the viability of TriMV.

4. Discussion

Viruses mount effective counterdefense strategies to overcome host defense mechanisms for replication and disease development (Anandalakshmi et al., 1998; Carrington et al., 2001). Encoding a VSR is the response of virus evolution to strong selection pressure exerted by host-induced antiviral RNA silencing. Several RNA viruses are known to

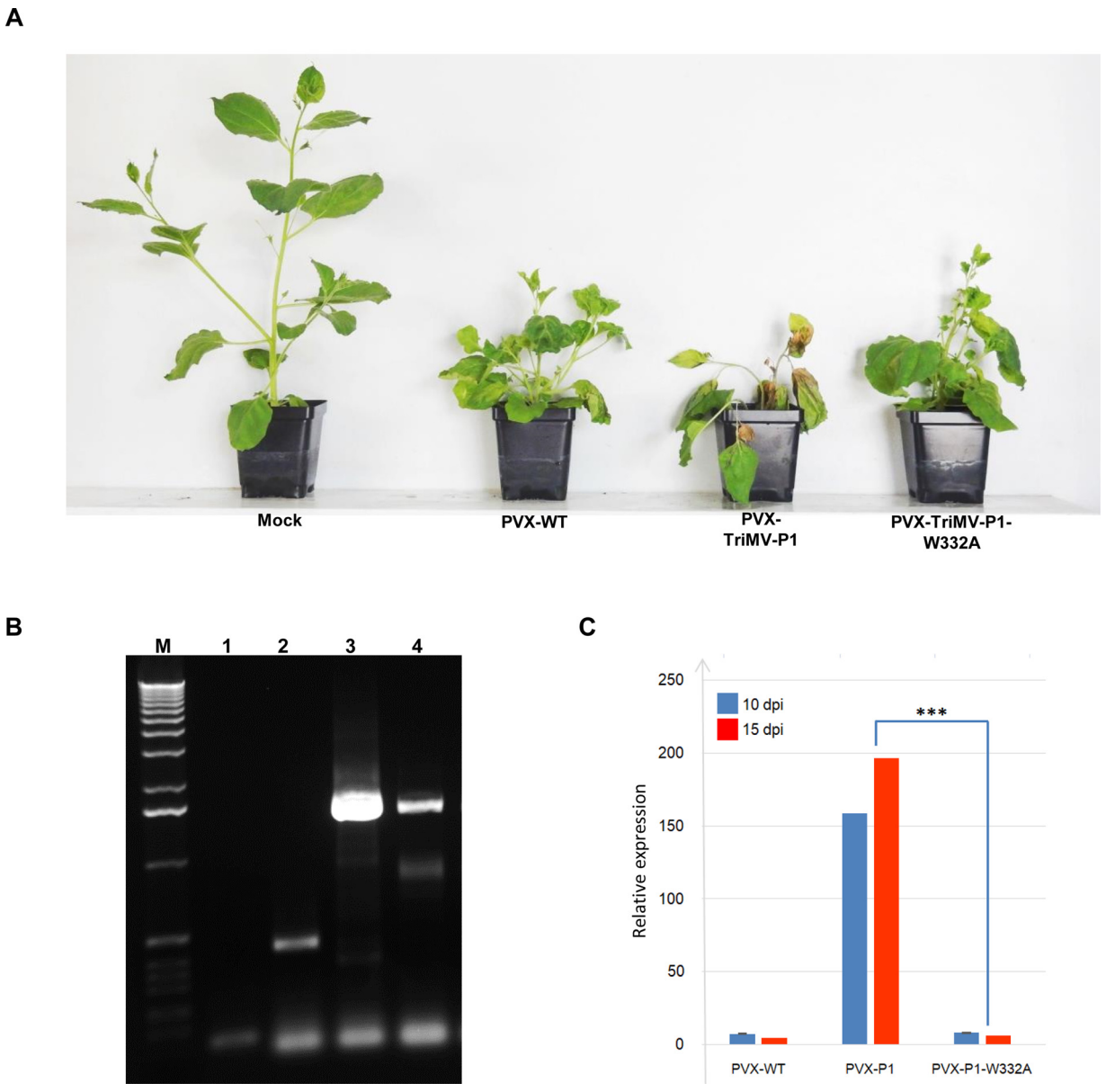

Fig. 6. The GW-motif in Triticum mosaic virus (TriMV) P1 is required for pathogenicity enhancement of potato virus X. (A) Symptom phenotypes of PVX-WT, PVX-TriMV-P1 and PVX-TriMV-P1-W332A on *N. benthamiana* plants at 15 days postinoculation (dpi). Note severe chlorosis and apical necrosis in PVX-TriMV-P1, but symptom recovery in PVX-TriMV-P1-W332A was similar to PVX-WT-infected plants. (B) RT-PCR analysis of insert stability in PVX-WT (lane 2), PVX-TriMV-P1 (lane 3) or PVX-TriMV-P1-W332A (lane 4) infected *N. benthamiana* plants at 15 dpi. Lane 1: Buffer-inoculated plants. Lane M represents 1.0 kbp DNA size marker. (C) Relative abundance of PVX transcripts assayed by real-time RT-PCR on total RNA extracted from symptomatic leaves. PVX-P1: PVX-TriMV-P1; PVX-P1-W332A: PVX-TriMV-P1-W332A. Internal reference of Nb-Actin was used to normalize PVX relative expression by ΔΔCt method. Most probable differences with 99% confidence represented as *** were calculated by Student's *T*-Test in each biological replicate. Error bars represent standard error.

encode VSRs, which evolved independently to outrun the evolutionary arms race with hosts (Li and Ding, 2006). We previously reported that the P1 protein of TriMV is a suppressor of RNA silencing (Tatineni et al., 2012). In this study, the domains and minimal regions of TriMV P1 required for VSR function were examined through deletion and alanine scanning analyses. Additionally, the mechanisms of viral suppression of RNA silencing employed by TriMV P1 were examined by using biochemical and *in vivo* studies.

Computational analyses of TriMV P1 sequence revealed the presence of conserved LXK/RA and zinc-finger domains toward the N-terminal region and a conserved domain harboring a GW-motif toward the C-terminal region. The N-terminal 50 amino acids are dispensable for VSR function, suggesting that these amino acids might be involved in other functions of the virus life-cycle such as replication, movement, or both. Deletion of 55 amino acids at the N-terminal region resulted in substantially reduced suppression of RNA silencing and additional deletions at the N-terminal region resulted in non-functional P1. These data suggest that P1 comprising 55–383 aa residues might harbor important motifs such as LXK/RA and zinc finger (Valli et al., 2008). Mutation of LR92/93 of LXK/RA motif completely abolished the suppression of RNA silencing function. Valli et al. (2011) found that mutations in LXK/RA motif abolished the suppression of RNA silencing activity and dsRNA binding function of CVYV P1b. It is possible that mutation of LXK/RA motif in TriMV P1 most likely abolished the dsRNA binding function. The zinc-finger like motif, $C_{110}X_2C_{113}X_nH_{127}X_2C_{130}$, is located in TriMV P1 between amino acids 110 and 130. Mutation of conserved amino acid residues in the putative zinc-finger domain either abolished or substantially reduced silencing

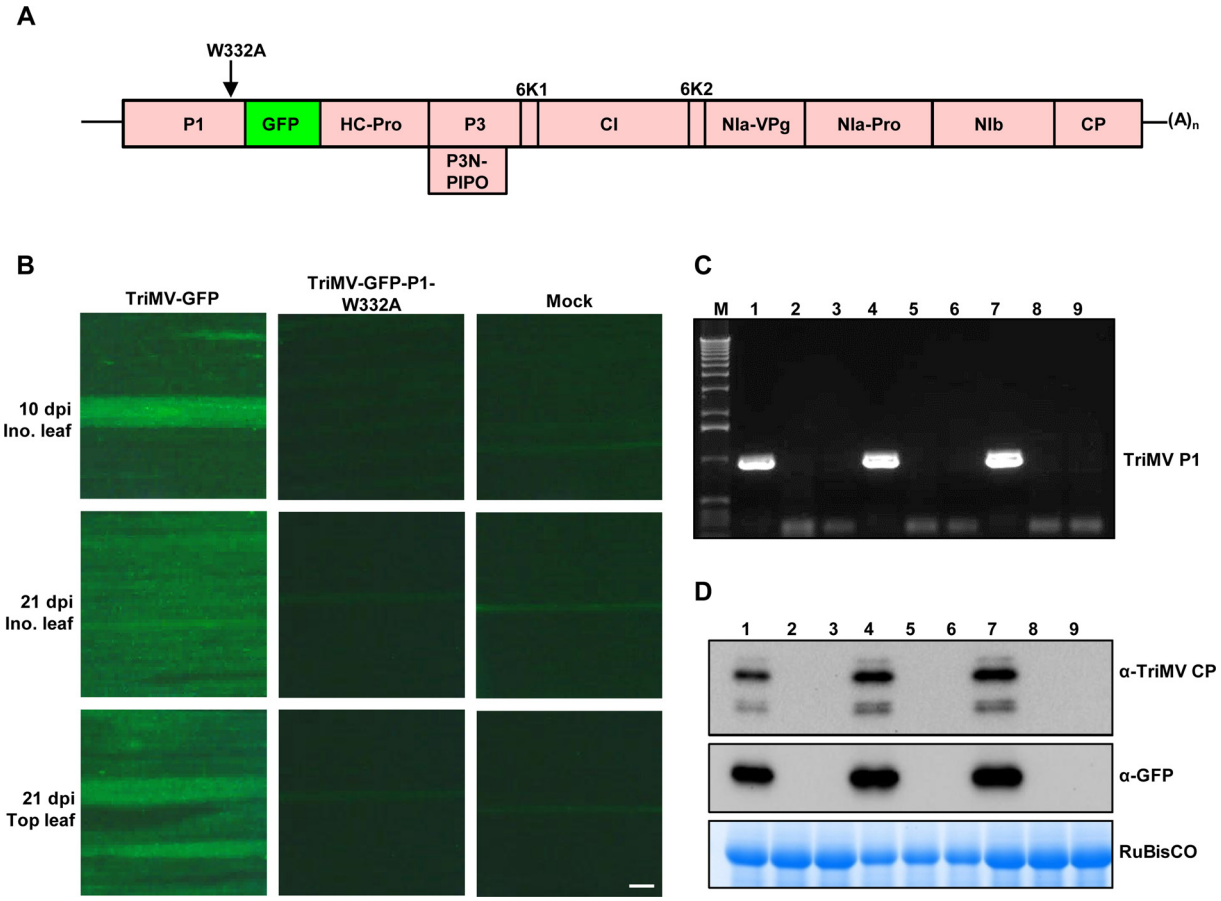

Fig. 7. Mutagenic disruption of the GW-motif in P1 cistron is lethal to Triticum mosaic virus (TriMV). (A) Genomic organization of GFP-tagged TriMV with W332A point mutation in P1 cistron. (B) Fluorescence micrographs (scale bar, 200 µm) of wheat leaves inoculated with *in vitro* transcripts as indicated. dpi: days post-inoculation. (C) RT-PCR assay for TriMV infection in wheat plants inoculated with *in vitro* transcripts of TriMV-GFP (lanes 1, 4, and 7), TriMV-W332A (lanes 2, 5, and 8), or buffer (lanes 3, 6, and 9) from inoculated leaves at 10 dpi (lanes 1–3) or 21 dpi (lanes 4–6) or upper noninoculated leaves at 21 dpi (lanes 7–9). Lane M represents 1.0 kbp DNA marker. (D) Western blot analysis on total proteins extracted from samples as in B to detect TriMV CP (top panel) or GFP (middle panel). RuBisCO panel (bottom) represents Coomassie Brilliant Blue R-250-stained SDS-PAGE indicating the amount of total protein loaded per well.

suppression activity of P1, suggesting that the zinc finger-like motif has a functional role in suppression of RNA silencing. Sequence conservation of LXK/RA and zinc finger-like domains in type B P1 proteins of silencing suppressors of *Poacevirus*, *Tritimovirus*, and *Ipomovirus* members, further emphasizes the functional role of these domains in combating host defense mechanisms.

Electrophoretic mobility shift assays were performed with bacterially expressed TriMV P1 protein as MBP fusion protein, which enhanced protein solubility (Pryor and Leiting, 1997). We found that P1 protein binds to 180-nt dsRNA as well as 21- and 24-nt ds-siRNAs, suggesting that TriMV P1 binds to dsRNAs in a size independent manner. The dsRNA binding property of P1 could potentially hurdle pre- and post-dicing stages of RNA silencing. Binding of P1 to long dsRNAs effectively protects the replicative form of viral RNAs from dicing machinery, thereby minimizing siRNA biogenesis. Sequestering 21- and 24-nt ds-siRNAs potentially cripples RISC formation (Mérai et al., 2006; Zilberman et al., 2003). The P1 proteins of TriMV and WSMV, suppressors of RNA silencing (Tatineni et al., 2012; Young et al., 2012), have been shown to possess dsRNA binding property (Gupta and Tatineni, 2019; this study). The dsRNA binding nature of TriMV P1 led to examine whether this protein protects long dsRNA from being diced into siRNAs by Dicer in an *in vitro* dicing reaction. The P1 protein effectively protected dsRNAs through binding, which was apparent from the electrophoretic mobility shift. Protection of dsRNA from *in vitro* dicing was evident with substantially reduced accumulation of diced product. However, accumulation of a few short dsRNAs in a dicing reaction with P1 might have resulted from the unbound fraction of dsRNA molecules available to Dicer enzyme. Additionally, TriMV P1 bound to dsRNAs derived from GFP (180 nt, 21 nt, and 24 nt) and TriMV CP (655 nt), suggesting sequence-independent nature of dsRNA binding.

Though TriMV P1 tolerated extensive deletions at the N-terminal region for VSR activity, only one C-terminal amino acid was dispensable. Recently, we found that WSMV P1 did not tolerate deletion of any amino acid at the C-terminus for suppression of RNA silencing function (Gupta and Tatineni, 2019). The plausible reason for this difference between TriMV and WSMV P1 proteins could be due to the presence of two C-terminal tyrosine residues in TriMV P1 but not in other P1 proteins (Fig. 5A; highlighted in yellow). The additional tyrosine residue in TriMV P1 might have compensated for the loss of a tyrosine residue at the C-terminus. Additionally, remarkable C-terminal sequence conservation among type B P1 proteins suggests minimal tolerance of mutations or deletions for suppression of RNA silencing.

A highly conserved GW dipeptide motif was found in all type B P1 sequences toward the C-terminal region with a potential role in suppression of RNA silencing. It has been reported that the host protein family GW182 is significant for facilitating slicer activity of PIWI (Ding and Han, 2007). Thus, the presence of the GW motif in P1 suggests steric inhibition of GW182 in AGO interaction except for direct AGO hooking (El-Shami et al., 2007). Szabó et al. (2012) found that the introduction of two additional GW motifs into the AGO-binding domain of sweet potato feathery mottle virus P1 converted it from a

nonfunctional suppressor to a functional suppressor with AGO binding capacity. These data suggest a functional role for WG/GW motifs in RNA silencing suppression function of type B P1 proteins of potyvirid species. Chou-Fasman's algorithm assigned a unique β-sheet to GW residing domain in the conceptual secondary structure of TriMV P1, and Kyte-Doolittle hydropathy scale measured the hydrophilicity of the GW microenvironment. Both of these suggest accessibility and solubility of the GW domain for intermolecular AGO interactions (Grishin, 2001; Shuryo, 1983; Watkins and Arora, 2014).

The role of the GW motif in TriMV P1 in virus biology was examined through a W332A mutation. Disruption of the GW motif abolished the suppression of RNA silencing activity, suggesting a functional role for this motif. Several VSRs have been shown to induce a disease phenotype when expressed through heterologous viruses (Ding et al., 1996). Previously, we have shown that PVX expressing TriMV P1 induced enhanced pathogenesis compared with wild-type PVX (Tatineni et al., 2012). In this study, we found that the GW motif was required for enhancement of pathogenicity as PVX harboring TriMV P1-W332A caused mild symptoms in *N. benthamiana* similar to that of wild-type PVX. Additionally, the role of the GW motif in TriMV biology was examined through a W332A mutation, and it was found that disruption of the GW motif abolished cell-to-cell movement in wheat. It is possible that the W332A mutation in the P1 cistron might have affected the proteinase activity of P1, which might have been lethal to TriMV. Nonetheless, disruption of the GW motif resulted in loss of RNA silencing suppression function and pathogenicity enhancement, a characteristic feature of most suppressors of RNA silencing. Taken together, our data suggest that the GW motif has a significant role in combating host defense mechanisms. Interestingly, disruption of the GW motif did not affect the dsRNA binding property of TriMV P1, suggesting that the GW motif most likely interacts with other host defense proteins to suppress RNA silencing.

Ethical approval

This article does not contain any studies with human participants or animals performed by any of the authors.

Acknowledgments

This work was funded by the United States Department of Agriculture-Agricultural Research Service Current Research Information System (5440-21000-033-00D). Mention of trade names or commercial products in this publication is solely for the purpose of providing specific information and does not imply recommendation or endorsement by the U.S. Department of Agriculture.

References

Anandalakshmi, R., Pruss, G.J., Ge, X., Marathe, R., Mallory, A.C., Smith, T.H., Vance, V.B., 1998. A viral suppressor of gene silencing in plants. Proc. Natl. Acad. Sci. U. S. A. 95, 13079–13084.

Bartel, D.P., 2004. MicroRNAs: genomics, biogenesis, mechanism, and function. Cell 116, 281–297.

Baulcombe, D., 2004. RNA silencing in plants. Nature 43, 356–363.

Béclin, C., Boutet, S., Waterhouse, P., Vaucheret, H., 2002. A branched pathway for transgene-induced RNA silencing in plants. Curr. Biol. 12, 684–688.

Bies-Etheve, N., Pontier, D., Lahmy, S., Picart, C., Vega, D., Cooke, R., Lagrange, T., 2009. RNA-directed DNA methylation requires an AGO4-interacting member of the SPT5 elongation factor family. EMBO Rep. 10, 649–654.

Buchon, N., Vaury, C., 2006. RNAi: a defensive RNA-silencing against viruses and transposable elements. Heredity (Edinb) 96, 195–202.

Burrows, M., Franc, G., Rush, C., Blunt, T., Ito, D., Kinzer, K., Olson, J., O'Mara, J., Price, J., Tande, C., Ziems, A., Stack, J., 2009. Occurrence of viruses in wheat in the Great Plains region, 2008. Plant Health Prog. https://doi.org/10.1094/PHP-2009-0706-01-RS. Online publication.

Byamukama, E., Tatineni, S., Hein, G.L., Graybosch, R.A., Baenziger, P.S., French, R., Wegulo, S.N., 2012. Effects of single and double infections of winter wheat by *Triticum mosaic virus* and *Wheat streak mosaic virus* on yield determinants. Plant Dis. 96, 859–864.

Byamukama, E., Seifers, D.L., Hein, G.L., De Wolf, E., Tisserat, N.A., Langham, M.A.C., Osborne, L.E., Timmerman, A., Wegulo, S.N., 2013. Occurrence and distribution of *Triticum mosaic virus* in the central Great Plains. Plant Dis. 97, 21–29.

Carrington, J.C., Freed, D.D., 1990. Cap-independent enhancement of translation by a plant potyvirus 5′ nontranslated region. J. Virol. 64, 1590–1597.

Carrington, J.C., Kasschau, K.D., Johansen, L.K., 2001. Activation and suppression of RNA silencing by plant viruses. Virology 281, 1–5.

Chapman, S., Kavanagh, T., Baulcombe, D.C., 1992. Potato virus X as a vector for gene expression in plants. Plant J. 2, 549–557.

Chiu, M.H., Chen, I.H., Baulcombe, D.C., Tsai, C.H., 2010. The silencing suppressor P25 of Potato virus X interacts with Argonaute1 and mediates its degradation through the proteasome pathway. Mol. Plant Pathol. 11, 641–649.

Chou, P.Y., Fasman, G.D., 1974. Conformational parameters for amino acids in helical, β-sheet, and random coil regions calculated from proteins. Biochemistry 13, 211–222.

Chuang, C.F., Meyerowitz, E.M., 2000. Specific and heritable genetic interference by double-stranded RNA in Arabidopsis thaliana. Proc. Natl. Acad. Sci. U. S. A. 97, 4985–4990.

Covey, S.N., Al-Kaff, N., Lángara, A., Turner, D.S., 1997. Plants combat infection by gene silencing. Nature 385, 781–782.

Csorba, T., Kontra, L., Burgyan, J., 2015. Viral silencing suppressors: tools forged to fine-tune host-pathogen coexistence. Virology 479–480, 85–103.

Deleris, A., Gallego-Bartolome, J., Bao, J., Kasschau, K.D., Carrington, J.C., Voinnet, O., 2006. Hierarchical action and inhibition of plant Dicer-like proteins in antiviral defense. Science 313, 68–71.

Diaz-Pendon, J.A., Li, F., Li, W.X., Ding, S.W., 2007. Suppression of antiviral silencing by cucumber mosaic virus 2b protein in Arabidopsis is associated with drastically reduced accumulation of three classes of viral small interfering RNAs. Plant Cell 19, 2053–2063.

Ding, L., Han, M., 2007. GW182 family proteins are crucial for microRNA-mediated gene silencing. Trends Cell Biol. 17, 411–416.

Ding, S.W., Voinnet, O., 2007. Antiviral immunity directed by small RNAs. Cell 130, 413–426.

Ding, S.W., Shi, B.J., Li, W.X., Symons, R.H., 1996. An interspecies hybrid RNA virus is significantly more virulent than either parental virus. Proc. Natl. Acad. Sci. U. S. A. 93, 7470–7474.

El-Shami, M., Pontier, D., Lahmy, S., Braun, L., Picart, C., Vega, D., Hakimi, M.A., Jacobsen, S.E., 2007. Cooke R, Lagrange T. Reiterated WG/GW motifs form functionally and evolutionarily conserved ARGONAUTE-binding platforms in RNAi-related components. Genes Dev. 21, 2539–2544.

Fellers, J.P., Seifers, D., Ryba-White, M., Martin, T.J., 2009. The complete genome sequence of Triticum mosaic virus, a new wheat-infecting virus of the High Plains. Arch. Virol. 154, 1511–1515.

Fire, A., Xu, S., Montgomery, M.K., Kostas, S.A., Driver, S.E., Mello, C.C., 1998. Potent and specific genetic interference by double-stranded RNA in Caenorhabditis elegans. Nature 391, 806–811.

Giner, A., Lakatos, L., García-Chapa, M., López-Moya, J.J., Burgyán, J., 2010. Viral protein inhibits RISC activity by argonaute binding through conserved WG/GW motifs. PLoS Pathog. 6, e1000996.

Grishin, N.V., 2001. Fold change in evolution of protein structures. J. Struct. Biol. 134, 167–185.

Guo, H., Song, X., Xie, C., Huo, Y., Zhang, F., Chen, X., Geng, Y., Fang, R., 2013. Rice yellow stunt rhabdovirus protein 6 suppresses systemic RNA silencing by blocking RDR6-mediated secondary siRNA synthesis. Mol. Plant Microbe Interact. 26, 927–936.

Gupta, A.K., Hein, G.L., Graybosch, R.A., Tatineni, S., 2018. Octapartite negative-sense RNA genome of High Plains wheat mosaic virus encodes two suppressors of RNA silencing. Virology 518, 152–162.

Gupta, A.K., Tatineni, S., 2019. Wheat streak mosaic virus P1 binds to dsRNAs without size and sequence specificity and a GW motif is crucial for suppression of RNA silencing. Viruses 11, 472.

Hamilton, A.J., Baulcombe, D.C., 1999. A species of small antisense RNA in post-transcriptional gene silencing in plants. Science 286, 950–952.

Henikoff, J.G., 1992. Amino acid substitution matrices from protein blocks. Proc. Natl. Acad. Sci. U. S. A. 89, 10915–10919.

Kasschau, K.D., Carrington, J.C., 1998. A counterdefensive strategy of plant viruses: suppression of posttranscriptional gene silencing. Cell 95, 461–470.

Kyte, J., Doolittle, R.F., 1982. A simple method for displaying the hydropathic character of a protein. J. Mol. Biol. 157, 105–132.

Lacombe, S., Bangratz, M., Vignols, F., Brugidou, C., 2010. The rice yellow mottle virus P1 protein exhibits dual functions to suppress and activate gene silencing. Plant J. 61, 371–382.

Lakatos, L., Csorba, T., Pantaleo, V., Chapman, E.J., Carrington, J.C., Liu, Y.P., Dolja, V.V., Calvino, L.F., Lopez-Moya, J.J., Burgyan, J., 2006. Small RNA binding is a common strategy to suppress RNA silencing by several viral suppressors. EMBO J. 25, 2768–2780.

Li, F., Ding, S.W., 2006. Virus counterdefense: diverse strategies for evading the RNA-silencing immunity. Annu. Rev. Microbiol. 60, 503–531.

McNeil, J.F., French, R., Hein, G.L., Baenziger, P.S., Askridge, K.M., 1996. Characterization of genetic variability among natural populations of Wheat streak mosaic virus. Phytopathology 86, 122–127.

Meister, G., Tuschl, T., 2004. Mechanisms of gene silencing by double-stranded RNA. Nature 431, 343–349.

Mérai, Z., Kerényi, Z., Molnár, A., Barta, E., Válóczi, A., Bisztray, G., Havelda, Z., Burgyán, J., Silhavy, D., 2005. Aureusvirus P14 is an efficient RNA silencing suppressor that binds double-stranded RNAs without size specificity. J. Virol. 79, 7217–7226.

Mérai, Z., Kerényi, Z., Kertész, S., Magna, M., Lakatos, L., Silhavy, D., 2006. Double-

stranded RNA binding may be a general plant RNA viral strategy to suppress RNA silencing. J. Virol. 80, 5747–5756.
Mingot, A., Valli, A., Rodamilans, B., Leon, D.S., Garcia, J.A., Lopez-Moya, J.J., 2016. The P1N-PISPO trans-frame gene of sweet potato feathery mottle potyvirus is produced during virus infection and functions as an RNA silencing suppressor. J. Virol. 90, 3543–3557.
Pryor, K.D., Leiting, B., 1997. High-level expression of soluble protein in Escherichia coli using a His6-tag and maltose-binding-protein double-affinity fusion system. Protein Expr. Purif. 10, 309–319.
Qu, F., Ren, T., Morris, T.J., 2003. The coat protein of turnip crinkle virus suppresses posttranscriptional gene silencing at an early initiation step. J. Virol. 77, 511–522.
Ratcliff, F., Harrison, B.D., Baulcombe, D.C., 1997. A similarity between viral defense and gene silencing in plants. Science 276, 1558–1560.
Rodamilans, B., Valli, A., Gacría, J.A., 2013. Mechanistic divergence between P1 proteases of the family Potyviridae. J. Gen. Virol. 94, 1407–1414.
Romano, N., Macino, G., 1992. Quelling: transient inactivation of gene expression in *Neurospora crassa* by transformation with homologous sequences. Mol. Microbiol. 6, 3343–3353.
Roth, B.M., Pruss, G.J., Vance, V.B., 2004. Plant viral suppressors of RNA silencing. Virus Res. 102, 97–108.
Ryan, M.D., Flint, M., 1997. Virus-encoded proteinases of the picornavirus super-group. J. Gen. Virol. 78, 699–723.
Samuel, G.H., Wiley, M.R., Badawi, A., Adelman, Z.N., Myles, K.M., 2016. Yellow fever virus capsid protein is a potent suppressor of RNA silencing that binds double-stranded RNA. Proc. Natl. Acad. Sci. U. S. A. 113, 13863–13868.
Schnettler, E., Hemmes, H., Huismann, R., Goldbach, R., Prins, M., Kormelink, R., 2010. Diverging affinity of tospovirus RNA silencing suppressor proteins, NSs, for various RNA duplex molecules. J. Virol. 84, 11542–11554.
Shi, B.J., Ding, S.W., Symons, R.H., 1997. Plasmid vector for cloning infectious cDNAs from plant RNA viruses: high infectivity of cDNA clones of tomato aspermy cucumovirus. J. Gen. Virol. 78, 1181–1185.
Shuryo, N., 1983. Structure-function relationships of food proteins with an emphasis on the importance of protein hydrophobicity. J. Agric. Food Chem. 31, 676–683.
Silhavy, D., Molnár, A., Lucioli, A., Szittya, G., Hornyik, C., Tavazza, M., Burgyán, J., 2002. A viral protein suppresses RNA silencing and binds silencing-generated, 21- to 25-nucleotide double-stranded RNAs. EMBO J. 21, 3070–3080.
Siomi, M.C., Sato, K., Pezic, D., Aravin, A.A., 2011. PIWI-interacting small RNAs: the vanguard of genome defence. Nat. Rev. Mol. Cell Biol. 12, 246–258.
Szabó, E.Z., Manczinger, M., Göblös, A., Kemény, L., Lakatos, L., 2012. Switching on RNA silencing suppressor activity by restoring Argonaute binding to a viral protein. J. Virol. 86, 8324–8327.
Tatineni, S., Ziems, A.D., Wegulo, S.N., French, R., 2009. *Triticum mosaic virus*: a distinct member of the Family *Potyviridae* with an unusually long leader sequence. Phytopathology 99, 943–950.
Tatineni, S., McMechan, J.A., Hein, G.L., French, R., 2011. Efficient and stable expression of GFP through *Wheat streak mosaic virus*-based vectors in cereal hosts using a range of cleavage sites: formation of dense fluorescent aggregates for sensitive virus tracking. Virology 410, 268–281.
Tatineni, S., Qu, F., Li, R., Morris, T.J., French, R., 2012. Triticum mosaic poacevirus enlists P1 rather than HC-Pro to suppress RNA silencing-mediated host defense. Virology 433, 104–115.
Tatineni, S., Sarath, G., Seifers, D., French, R., 2013. Immunodetection of Triticum mosaic virus by DAS- and DAC-ELISA using antibodies produced against coat protein expressed in Escherichia coli: potential for high-throughput diagnostic methods. J. Virol. Methods 189, 196–203.
Tatineni, S., McMechan, A.J., Bartels, M., Hein, G.L., Graybosch, R.A., 2015. *In vitro* transcripts of wild-type and fluorescent protein-tagged *Triticum mosaic virus* (family *Potyviridae*) are biologically active in wheat. Phytopathology 105, 1496–1505.
Ullu, E., Tschudi, C., Chakraborty, T., 2004. RNA interference in protozoan parasites. Cell. Microbiol. 6, 509–519.
Untiveros, M., Olspert, A., Artola, K., Firth, A.E., Kreuze, J.F., Valkonen, J.P.T., 2016. A novel sweet potato potyvirus open reading frame (ORF) is expressed vial polymerase slippage and suppresses RNA silencing. Mol. Plant Pathol. 17, 1111–1123.
Valli, A., Martín-Hernández, A.M., López-Moya, J.J., García, J.A., 2006. RNA silencing suppression by a second copy of the P1 serine protease of Cucumber vein yellowing ipomovirus, a member of the family *Potyviridae* that lacks the cysteine protease HC-Pro. J. Virol. 80, 10055–10063.
Valli, A., Dujovny, G., Garcia, J.A., 2008. Protease activity, self-interaction, and small interfering RNA binding of the silencing suppressor P1b from cucumber vein yellowing Ipomovirus. J. Virol. 82, 974–986.
Valli, A., Oliveros, J.C., Molnar, A., Baulcombe, D.C., Garcia, J.A., 2011. The specific binding to 21-nt double-stranded RNAs is crucial for the anti-silencing activity of cucumber vein yellowing virus P1b and perturbs endogenous small RNA populations. RNA 17, 1148–1158.
Valli, A.A., Gallo, G., Rodamilans, B., López-Moya, J.A., García, J.A., 2018. The HC-Pro from the *Potyviridae* family: an enviable multitasking helper component that every virus would like to have. Mol. Plant Pathol. 19, 744–763.
Verchot, J., Koonin, E.V., Carrington, J.C., 1991. The 35-kDa protein from the N-terminus of the potyviral polyprotein functions as a third virus-encoded proteinase. Virology 18, 527–535.
Verchot, J., Herndon, K.L., Carrington, J.C., 1992. Mutational analysis of the tobacco etch potyviral 35-kDa proteinase: identification of essential residues and requirements for autoproteolysis. Virology 190, 298–306.
Voinnet, O., Baulcombe, D.C., 1997. Systemic signaling in gene silencing. Nature 389, 553.
Watkins, A.M., Arora, P.S., 2014. Anatomy of β-strands at protein-protein interfaces. ACS Chem. Biol. 9, 1747–1754.
Xie, Z., Fan, B., Chen, C., Chen, Z., 2001. An important role of an inducible RNA-dependent RNA polymerase in plant antiviral defense. Proc. Natl. Acad. Sci. U. S. A. 98, 6516–6521.
Young, B.A., Stenger, D.C., Qu, F., Morris, T.J., Tatineni, S., French, R., 2012. Tritimovirus P1 functions as a suppressor of RNA silencing and an enhancer of disease symptoms. Virus Res. 163, 672–677.
Zilberman, D., Cao, X., Jacobsen, S.E., 2003. ARGONAUTE4 control of locus-specific siRNA accumulation and DNA and histone methylation. Science 299, 716–719.